

# ASMOP: Additional sampling stochastic trust region method for multi-objective problems

Nataša Krklec Jerinkić <sup>\*</sup>; Luka Rutešić <sup>†‡</sup>; Ilaria Trombini <sup>§</sup>

## Abstract

We consider unconstrained multi-criteria optimization problems with finite sum objective functions. The proposed algorithm belongs to a non-monotone trust region framework where additional sampling approach is used to govern the sample size and the acceptance of a candidate point. Depending on the problem, the method can yield a mini-batch or an increasing sample size behavior. This work can be viewed as an extension of additional sampling trust region method for scalar finite sum function minimization presented in the literature, requiring nontrivial modifications both in construction and in convergence analysis of the algorithm. Under assumptions standard for this framework, we prove stochastic convergence for twice continuously-differentiable, but possibly non-convex objective functions. The experiments on machine learning binary classification datasets show the efficiency of the proposed scheme and its competitiveness with the relevant state-of-the-art methods in both convex and non-convex setup.

**Key words:** Additional sampling, non-monotone trust region, adaptive sample size, multi-objective optimization, Pareto critical points, stochastic convergence.

## 1 Introduction

The problem we are solving can be stated as

$$\min_{x \in \mathbb{R}^n} f(x) := (f^1(x), \dots, f^q(x))^T \quad (1)$$

---

<sup>\*</sup>Department of Mathematics and Informatics, Faculty of Sciences, University of Novi Sad, Trg Dositeja Obradovića 4, 21000 Novi Sad, Serbia. e-mail: [natasa.krklec@dmi.uns.ac.rs](mailto:natasa.krklec@dmi.uns.ac.rs)

<sup>†</sup>Department of Mathematics and Informatics, Faculty of Sciences, University of Novi Sad, Trg Dositeja Obradovića 4, 21000 Novi Sad, Serbia. e-mail: [luka.rutesic@dmi.uns.ac.rs](mailto:luka.rutesic@dmi.uns.ac.rs)

<sup>‡</sup>Corresponding author

<sup>§</sup>Department of Mathematics and Computer Science, University of Ferrara, Via Machiavelli 30, 44121 Ferrara, Italy. e-mail: [ilaria.trombini@unife.it](mailto:ilaria.trombini@unife.it)

where  $f : R^n \rightarrow R^q$  and each component function is assumed to be smooth with Lipschitz-continuous gradients. Let  $\mathcal{N}^i$ ,  $i = 1, \dots, q$  be the respective index sets and  $N^i = |\mathcal{N}^i| = N$ , for all  $i = 1, \dots, q$ . We assume that each component function has the following finite sum form

$$f^i(x) := \frac{1}{N} \sum_{j \in \mathcal{N}^i} f_j^i(x), \quad i = 1, \dots, q. \quad (2)$$

This setup is often encountered in Machine Learning (ML) and Deep Learning (DL) and it has been widely researched, yielding many crafty optimization methods. The considered problems are often nonlinear, nonconvex, and large-scale, which calls for the development of stochastic optimization methods specialized for Multi-Objective (MO) problems. In ML terms, each component function  $f^i(x)$  can be seen as a distinct average loss function, where  $x \in R^n$  is the vector of trainable parameters for input-label pairs  $\{(a_j^i, y_j^i)\}_{j=1}^N$  of the training dataset, i.e.,

$$f_j^i(x) := L^i(a_j^i, y_j^i; x), \quad j = 1, \dots, N, i = 1, \dots, q,$$

and  $L^i(\cdot)$  measures the prediction error. For the method we propose, the stochastic inflow comes from subsampling which is used to reduce the computational costs of evaluating the full functions (2) and possibly the relevant derivatives.

The points of interest in multi-criteria problems are Pareto critical points which cannot be locally improved in terms of all component function values [10],[23]. Finding Pareto critical points yields possibility of finding an entire Pareto front - a set of globally optimal points [9]. This is extremely important in some applications since the representation of the entire front can provide crucial information. Pareto critical points can be characterized as zeros of the so called marginal function (see [10] for more details). In the single-objective case ( $q = 1$ ), this concept is reduced to the well known first order optimality conditions, i.e., finding a stationary point of the objective function. Therefore, a common approach in the analysis of multi-criteria optimization is to show that (sub)sequence of marginal function values converges to zero. In stochastic setup, where only approximate values of the functions and the derivatives are available, the approximate marginal function plays a significant role in the algorithm, while the analysis aims stochastic convergence of the true marginal function [26],[17]

Both the line search and the trust region approach has been researched in multi-objective optimization, resulting in a number of deterministic and stochastic algorithms. Deterministic multi-criteria steepest descent and Newton method, together with a projected gradient method for the constrained case has been discussed in [11]. The stochastic multi-gradient, an extension of the classical stochastic gradient (SG) [21], can be found in [20],

in which sublinear convergence for convex and strongly convex functions is shown.

In [27], the marginal function is utilized to define the trust region method, and therein a convergence towards a critical point is shown. The complexity of multi-objective problems motivates the development of the stochastic and derivative free approaches. In [26], a black box function is used and the derivative is unknown. Therein it is shown that by using the true function values and approximate derivatives it is possible to prove convergence towards a Pareto optimal point. It is also possible to use both approximate function and gradient values if the estimates are sufficiently accurate with high probability (probabilistically fully linear), see [17], which is a generalization of [8]. Therein, an adaptive subsampling technique is used which depends on the trust region radius. It successfully reduced the computational cost by using less data when the radius is larger.

The literature also provides methods designed for problems with the finite sum objective functions. These methods exploit the structure of the function and their advantage lies in subsampling techniques. It is shown that subsampling can help in reducing the costs of deterministic schemes where the full sample set is needed at all iterations, yielding excessive optimization costs. Some papers on this topic are [1],[2],[3],[4],[5],[6],[22]. Moreover, sampling is inevitable in infinite sum problems that are used for modeling online training process, or in more general problems where the objective function is in a form of mathematical expectation (see [15] or [19] for instance). In [13] an additional sampling technique is employed within a non-monotone trust region framework, aiming to solve single-criterion problems. The idea of non-monotonicity within trust region framework is also present in the literature [28],[25],[7].

In this work, we propose a stochastic non-monotone trust region algorithm for solving multi-objective problems (1)-(2). At each iteration we employ subsampled functions and gradients to find a candidate subsequent point based on approximate trust region model. The acceptance of that point is based on additional sampling technique [13],[18],[12], [24], which also governs the subsampling strategy. This means that besides subsampling needed to form an approximate model and the candidate point, we also use an independent subsampled functions as a decision making criteria. Roughly speaking, the role of additional sampling is to test the heterogeneity of the data and increase the level of precision if necessary. By adaptively choosing the sample size for each component, we handle the sample average approximation error for each objective function separately. This leads to two different sample size scenarios: 1) “mini-batch scenario”, where at least one of the objective functions is approximated during the whole optimization process; and 2) “full sample scenario”, where the full sample is reached eventually for all the objective functions.

In particular, the presented work generalizes the additional sampling

non-monotone trust region approach for single-objective problems [13] to multi-objective setup. This adaptation requires nontrivial modifications both in the algorithm's construction and in the convergence analysis. The resulting method yields adaptive sample size sequences designed to reduce costs by exploiting the problem's structure, while ensuring the convergence towards critical points under some common assumptions for this setup, regardless of the sample size scenario.

The paper is organized as follows. Some basic concepts are covered in the following section. Section 3 presents the proposed algorithm. Within Section 4 the stochastic convergence of the proposed method is analyzed, while Section 5 is devoted to numerical results. Some conclusions are drawn in Section 6.

## 2 Preliminaries

We start this section by defining efficient and weakly efficient solutions of problem (1).

**Definition 1.** [10] A point  $x^* \in \mathbb{R}^n$  is called (an) efficient (solution) for (1) (or Pareto optimal) if there exists no point  $x \in \mathbb{R}^n$  satisfying  $f^i(x) \leq f^i(x^*)$  for all  $i \in \{1, 2, \dots, q\}$  and  $f(x) \neq f(x^*)$ . A point  $x^* \in \mathbb{R}^n$  is called (a) weakly efficient (solution) for (1) (or weakly Pareto optimal) if there exists no point  $x \in \mathbb{R}^n$  satisfying  $f^i(x) < f^i(x^*)$  for all  $i \in \{1, 2, \dots, q\}$ .

It can be shown that a stationarity condition for problem (1) is related to marginal function

$$\omega(x) = - \min_{\|d\| \leq 1} \left( \max_{i \in \{1, \dots, q\}} \langle \nabla f^i(x), d \rangle \right). \quad (3)$$

Notice that  $\omega(x) = \|\nabla f(x)\|$  if  $q = 1$  since the solution of problem (3) is  $d^{opt}(x) = -\nabla f(x)/\|\nabla f(x)\|$  in that case. In general, marginal function characterizes Pareto critical points as stated in the following lemma.

**Lemma 1.** [10] Let  $\mathcal{D}(x)$  be the set of solutions of (3). Then

- a)  $\omega(x) \geq 0$ , for every  $x \in \mathbb{R}^n$ ;
- b) if  $x$  is Pareto critical for (1) then  $0 \in \mathcal{D}(x)$  and  $\omega(x) = 0$ ;
- c) if  $x$  is not Pareto critical of (1) then  $\omega(x) > 0$  and any  $d \in \mathcal{D}(x)$  is a descent direction for (1);
- d) the mapping  $x \rightarrow \omega(x)$  is continuous.

One possible scalar representation of the multi-objective problem (1) is

$$\min_{x \in \mathbb{R}^n} \phi(x), \quad \phi(x) := \max_{i \in \{1, \dots, q\}} f^i(x). \quad (4)$$

Although problems (1) and (4) are not equivalent, it can be shown that every solution problem (4) is a Pareto critical point of problem (1).

At each iteration  $k$  we form a sample average approximations of functions (2) and their derivatives as follows

$$f_{\mathcal{N}_k^i}^i(x) = \frac{1}{N_k^i} \sum_{j \in \mathcal{N}_k^i} f_j^i(x), \quad \nabla f_{\mathcal{N}_k^i}^i(x) = \frac{1}{N_k^i} \sum_{j \in \mathcal{N}_k^i} \nabla f_j^i(x), \quad (5)$$

where  $\mathcal{N}_k^i \subseteq \mathcal{N}^i$  and  $N_k^i = |\mathcal{N}_k^i|$ . Moreover, we consider the approximate marginal functions [26]

$$\omega_{\mathcal{N}_k}(x) = - \min_{\|d\| \leq 1} \left( \max_{i \in \{1, \dots, q\}} \langle \nabla f_{\mathcal{N}_k^i}^i(x), d \rangle \right) \quad (6)$$

where  $\mathcal{N}_k = (\mathcal{N}_k^1, \dots, \mathcal{N}_k^q) \subseteq \mathcal{N} = (\mathcal{N}^1, \dots, \mathcal{N}^q)$  is the set  $q$ -tuple. The corresponding scalar problem is then given by

$$\min_{x \in \mathbb{R}^n} \phi_{\mathcal{N}_k}(x), \quad \phi_{\mathcal{N}_k}(x) := \max_{i \in \{1, \dots, q\}} f_{\mathcal{N}_k^i}^i(x). \quad (7)$$

Following the ideas from deterministic setup, we form a quadratic model of (7) as

$$m_{\mathcal{N}_k}(d) = \max_{i \in \{1, \dots, q\}} m_{\mathcal{N}_k^i}(d), \quad (8)$$

$$m_{\mathcal{N}_k^i}(d) := f_{\mathcal{N}_k^i}^i(x_k) + \langle \nabla f_{\mathcal{N}_k^i}^i(x_k), d \rangle + \frac{1}{2} \langle d, H_k^i d \rangle,$$

where  $H_k^i$  approximates the Hessian of function  $f^i$  for  $i = 1, \dots, q$  at iteration  $k$ . Notice that for each  $i = 1, \dots, q$ ,  $\nabla m_{\mathcal{N}_k^i}(0) = \nabla f_{\mathcal{N}_k^i}^i(x_k)$ , and  $m_{\mathcal{N}_k^i}(0) = f_{\mathcal{N}_k^i}^i(x_k)$ .

Furthermore, following the approach of [13], we will rely on additional sampling and draw independently sampled subsets to govern sampling strategy of the method. This yields a nondecreasing, adaptive subsampling approach constructed in a such way to avoid employing the entire sample set for functions  $f^i$  which are homogeneous, i.e., whose subsampled values do not noticeably differ from the full sample values. On the other hand, if the local functions of an objective  $f^i$  are heterogeneous, mini-batch does not provide a good representative and the sample size is increased gradually. As mentioned, this will create two possible scenarios: “mini-batch” (MB) and “full sample” (FS). Recall that in the MB scenario, there exists at least one component function  $f^i$  for which the subsampling size  $N_k^i$  is strictly less than the full sample size  $N$  throughout the algorithm. On the other hand, FS

does not imply fully deterministic approach, but rather a non-monotonically increasing sample mode where the full sample is reached eventually. More formally, let us define

$$M_b := \{i \in \{1, \dots, q\} \mid N_k^i < N, \forall k \in \mathbb{N}\}. \quad (9)$$

Thus,  $M_b \neq \emptyset$  implies MB scenario, while  $M_b = \emptyset$  implies FS scenario. Notice that scenario depends on a sample path - the outcome of the algorithm influenced by random sampling. Denoting the set of all possible sample paths of the algorithm by  $\Omega$ , we have  $\Omega = MB \cup FS$  and  $MB \cap FS = \emptyset$ , where  $MB \subseteq \Omega$  represents all possible sample paths such that  $M_b \neq \emptyset$ , while  $FS \subseteq \Omega$  represents all possible sample paths such that  $M_b = \emptyset$ .

### 3 Algorithm

Within this section we present Additional Sampling algorithm for Multi-Objective Problems - ASMOP. As mentioned earlier, at each iteration  $k$ , a quadratic model  $m_{\mathcal{N}_k}(d)$  is formed using the subsampled values (5) and Hessian approximations  $H_k^i$ . Then, the direction is obtained by solving the following problem approximately

$$\min_{\|d\| \leq \delta_k} m_{\mathcal{N}_k}(d), \quad (10)$$

where  $\delta_k$  is the trust region radius. The approximate solution  $d_k$  is such that the Cauchy decrease condition holds

$$m_{\mathcal{N}_k}(0) - m_{\mathcal{N}_k}(d_k) \geq \frac{1}{2} \omega_{\mathcal{N}_k}(x_k) \min\{\delta_k, \frac{\omega_{\mathcal{N}_k}(x_k)}{\beta_k}\} \quad (11)$$

with

$$\beta_k = 1 + \max_{i \in \{1, \dots, q\}} \|H_k^i\|. \quad (12)$$

It can be shown that such direction exists (see Lemma 2 of [17] for instance). Similar to [13], we will define a trial point  $x_t = x_k + d_k$ , and check the ratio between the decrease of the relevant scalar function and the quadratic model. Since we are dealing with noisy approximations in general, we adopt non-monotone trust region strategy to avoid imposing a strict decrease and define the ratio as follows

$$\rho_{\mathcal{N}_k} := \frac{\phi_{\mathcal{N}_k}(x_t) - \phi_{\mathcal{N}_k}(x_k) - \delta_k t_k}{m_{\mathcal{N}_k}(d_k) - m_{\mathcal{N}_k}(0)} \quad (13)$$

where  $t_k > 0$  for all  $k$  and

$$\sum_{k=0}^{\infty} t_k \leq t < \infty. \quad (14)$$

The role of  $t_k$  is to control a potential increase of the scalar function and it is assumed to be predetermined.

Furthermore, let us define the set of indices at iteration  $k$  for which we have an approximate function values, i.e.,

$$M_b^k := \{i \in \{1, \dots, q\} \mid N_k^i < N\}. \quad (15)$$

If  $M_b = \emptyset$  then we say that the algorithm is in the FS (full sample) phase at iteration  $k$ . On the other hand, we say that the algorithm is in the MB (mini-batch) phase at iteration  $k$  if  $M_b \neq \emptyset$ . If we are in the MB phase, the independent additional sampling is performed. More precisely, we sample  $\mathcal{D}_k = (\mathcal{D}_k^1, \dots, \mathcal{D}_k^q)$ , independently of  $\mathcal{N}_k$ , with  $\mathcal{D}_k^i \subset \mathcal{N}^i$  such that  $D_k^i = |\mathcal{D}_k^i| < N$  for all  $i = 1, \dots, q$ . The subsample  $\mathcal{D}_k$  is used to calculate  $f_{\mathcal{D}_k^i}^i(x_k)$ ,  $f_{\mathcal{D}_k^i}^i(x_t)$  and  $\nabla f_{\mathcal{D}_k^i}^i(x_k)$  by the following formulas

$$f_{\mathcal{D}_k^i}^i(x) = \frac{1}{D_k^i} \sum_{j \in \mathcal{D}_k^i} f_j^i(x), \quad \nabla f_{\mathcal{D}_k^i}^i(x) = \frac{1}{D_k^i} \sum_{j \in \mathcal{D}_k^i} \nabla f_j^i(x), \quad i = 1, \dots, q. \quad (16)$$

Keep in mind that it is possible that some component functions reached the full sample, while the others did not. For each  $i \notin M_b^k$  we set  $\mathcal{D}_k^i = \mathcal{N}^i$ , i.e., we have  $f_{\mathcal{D}_k^i}^i(x) = f_{\mathcal{N}_k^i}^i(x) = f_{\mathcal{N}^i}^i(x)$ . For all the other components  $i \in M_b^k$  it is possible to use subsamples  $\mathcal{D}_k^i$  of arbitrary small sizes. In our experiments we set  $D_k^i = 2$ , which keeps the computational cost of additional sampling low.

The following ratio acts as an additional measure of adequacy of the trial point

$$\rho_{\mathcal{D}_k} := \frac{\phi_{\mathcal{D}_k}(x_t) - \phi_{\mathcal{D}_k}(x_k) - \delta_k \bar{t}_k}{-\max_{i \in \{1, \dots, q\}} \|\nabla f_{\mathcal{D}_k^i}^i(x_k)\|} \quad (17)$$

where  $\phi_{\mathcal{D}_k}(x) := \max_{i \in \{1, \dots, q\}} f_{\mathcal{D}_k^i}^i(x)$ ,  $\bar{t}_k > 0$  and

$$\sum_{k=0}^{\infty} \bar{t}_k \leq \bar{t} < \infty. \quad (18)$$

Notice that  $\rho_{\mathcal{D}_k} \geq \nu$  is equivalent to an Armijo-like condition

$$\phi_{\mathcal{D}_k}(x_t) \leq \phi_{\mathcal{D}_k}(x_k) + \delta_k \bar{t}_k - \nu \max_{i \in \{1, \dots, q\}} \|\nabla f_{\mathcal{D}_k^i}^i(x_k)\|. \quad (19)$$

In the MB phase, the trial point is accepted if both  $\rho_{\mathcal{N}_k} \geq \eta$  and  $\rho_{\mathcal{D}_k} \geq \nu$ . Notice that the second condition may be very strong since the maximum of the approximate gradients appears on the right-hand side of (19). This is balanced with the choice of predetermined non-monotonicity parameter sequence  $\{\bar{t}_k\}$ . The ratio  $\rho_{\mathcal{D}_k}$  also plays a significant role in subsampling strategy as will be seen within the algorithm. Therefore, the choice of the

non-monotonicity parameter may have a big impact on the algorithm's behavior as will be demonstrated within Section 5. If ASMOP reaches the FS phase, only  $\rho_{\mathcal{N}_k} = \rho_{\mathcal{N}}$  is considered as in the deterministic version of the multi objective trust region [27].

One more mechanism is used to control the sample size behavior. Namely, if we get relatively close to Pareto critical point on an approximate problem, more precisely, if  $\omega_{\mathcal{N}_k}(x_k) < \varepsilon h_k^i$  where

$$h_k^i := \frac{N - N_k^i}{N} \quad (20)$$

is a sample average approximation error estimate, we increase the subsampling size. The algorithm can be stated as follows.

**Algorithm 1.** (*ASMOP*)

Step 0. *Initialization.*

Choose  $x_0 \in \mathbb{R}^n$ ,  $\delta_{max} > 0$ ,  $\delta_0 \in (0, \delta_{max})$ ,  $\gamma_1 \in (0, 1)$ ,  $\gamma_2 = 1/\gamma_1$ ,  $\nu, \varepsilon > 0$ ,  $\eta \in (0, \frac{3}{4})$ ,  $\{t_k\}$  satisfying (14) and  $\{\bar{t}_k\}$  satisfying (18),  $\mathcal{N}_0 = (\mathcal{N}_0^1, \dots, \mathcal{N}_0^q)$ . Set  $k = 0$ .

Step 1. *Candidate point.*

Form the model (8) and find the step such that (11) holds.

Calculate  $\rho_{\mathcal{N}_k}$  by (13) and  $\omega_{\mathcal{N}_k}(x_k)$  by (6).

Set  $x_t = x_k + d_k$ .

Step 2. *Sample update.*

**if**  $M_b^k = \emptyset$  (**FS phase**) **then**

Go to Step 3.

**else** (**MB phase**)

For all  $i \in M_b^k$ :

Choose  $\mathcal{D}_k^i$  randomly and uniformly, with replacement, from  $\mathcal{N}^i$  and calculate  $\rho_{\mathcal{D}_k}$  by (17).

**if**  $\omega_{\mathcal{N}_k}(x_k) < \varepsilon h_k^i$  **then**

Choose  $N_{k+1}^i \in (N_k^i, N]$  and choose  $\mathcal{N}_{k+1}^i$ .

**else**

**if**  $\rho_{\mathcal{D}_k} < \nu$  **then**

Choose  $N_{k+1}^i \in (N_k^i, N]$  and choose  $\mathcal{N}_{k+1}^i$ .

**else**

**if**  $\rho_{\mathcal{N}_k} < \eta$  **then**

Set  $N_{k+1}^i = N_k^i$  and  $\mathcal{N}_{k+1}^i = \mathcal{N}_k^i$ .

**else**

Set  $N_{k+1}^i = N_k^i$ , and choose  $\mathcal{N}_{k+1}^i$ .

**end if**

**end if**

**end if**

**end if**

Step 3. *Iterate update.*

```

if  $M_b^k \neq \emptyset$  (MB phase) then
  if  $\rho_{\mathcal{N}_k} \geq \eta$  and  $\rho_{\mathcal{D}_k} \geq \nu$  then
     $x_{k+1} = x_t$ .
  else
     $x_{k+1} = x_k$ .
  end if
else (FS phase)
  if  $\rho_{\mathcal{N}_k} \geq \eta$  then
     $x_{k+1} = x_t$ .
  else
     $x_{k+1} = x_k$ .
  end if
end if

```

Step 4. *Radius update.*

```

if  $\rho_{\mathcal{N}_k} \geq \eta$  then
   $\delta_{k+1} = \min\{\delta_{max}, \gamma_2 \delta_k\}$ .
else
   $\delta_{k+1} = \gamma_1 \delta_k$ .
end if

```

Step 5. *Counter update.*

Set  $k = k + 1$  and go to Step 1.

A few more words are due to algorithm's construction. The initialization includes setting the hyper-parameters, including the trust region radius bound  $\delta_{max}$  and the initial sample size  $\mathcal{N}_0$ . Step 1 finds a candidate point through finding a suitable direction  $d_k$  based on the chosen sample  $\mathcal{N}_k$ . We also calculate the corresponding approximate marginal function.

Notice that Step 2 is relevant only if the MB phase is active and it is devoted to the sample  $\mathcal{N}_k$  update. Besides determining the sample size  $N_{k+1}$  to be used in the next iteration, we also determine whether the same sample should be retained. The additional sample  $\mathcal{D}_k$  is drawn according to the stated rules to ensure theoretical requirements. Recall that the sample size of  $D_k^i$  can be arbitrarily small for all  $i$  and  $k$ . The independence from  $\mathcal{N}_k$  is crucial since we need an independent "second opinion" on the trial point.

The sample size can be increased due to  $\omega_{\mathcal{N}_k}(x_k) < \varepsilon h_k^i$  or  $\rho_{\mathcal{D}_k} < \nu$ . The later case indicates that the trial point obtained via  $\mathcal{N}_k$  is a bad choice with respect to independent representative  $\phi_{\mathcal{D}_k}$  of the original scalar representation  $\phi$ . This signals potential heterogeneity of the data and requirement for a better approximation by employing a larger subsample. If both  $\omega_{\mathcal{N}_k}(x_k) \geq \varepsilon h_k^i$  and  $\rho_{\mathcal{D}_k} \geq \nu$  hold, then we check the agreement  $\rho_{\mathcal{N}_k}$ . If  $\rho_{\mathcal{N}_k} < \eta$  then we suspect that the model  $m_{\mathcal{N}_k}$  was not good enough approximation of  $\phi_{\mathcal{N}_k}$  and that the failure was due to inadequate radius rather

than inadequate sample. In that case, we keep the same sample size, but also retain the same sample for the next iteration. Finally, if the agreement is good enough, i.e.,  $\rho_{\mathcal{N}_k} \geq \eta$ , we proceed with the same sample size, but with a different sample. Notice that the sample size sequence is nondecreasing. Therefore, if the algorithm enters the FS phase, it remains in it until the end.

Step 3 is devoted to the acceptance of the trial point. In the MB phase, both measures of agreement  $\rho_{\mathcal{N}_k}$  and  $\rho_{\mathcal{D}_k}$  need to be big enough in order to accept the trial point, while in the FS phase the decision is reduced to  $\rho_{\mathcal{N}_k}$ . The trust region radius is updated within Step 4 where the decision is based solely on  $\rho_{\mathcal{N}_k}$  regardless of the phase of the algorithm.

## 4 Convergence analysis

Within this section we prove almost sure convergence of a subsequence of marginal functions  $\omega(x_k)$ , which is an equivalent of vanishing subsequence of gradients in the scalar case ( $q = 1$ ). We start the analysis by imposing some standard assumptions for the considered framework.

**Assumption 1.** All the functions  $f_j^i$ ,  $j \in \mathcal{N}^i$ ,  $i = 1, \dots, q$  are twice continuously differentiable and bounded from below.

Notice that this assumption implies that all the subsampled functions  $f_{\mathcal{N}_k}^i$ ,  $i = 1, \dots, q$  are twice continuously differentiable and bounded from below as well.

**Assumption 2.** There exists a positive constant  $c_h$  such that

$$\|\nabla^2 f_j^i(x)\| \leq c_h \quad \text{for all } x \in \mathbb{R}^n, j \in \mathcal{N}^i, i = 1, \dots, q,$$

and the sequence of  $\beta_k$  defined by (12) is uniformly bounded, i.e., there exists a positive constant  $c_b$  such that

$$\beta_k = 1 + \max_i \|H_k^i\| \leq c_b \quad \text{for all } k \in \mathbb{N}.$$

This assumption implies that all the Hessians  $\|\nabla^2 f_{\mathcal{N}_k}^i(x)\|$  are uniformly bounded as well with the same constant  $c_h$ . Although restrictive, this assumption is satisfied in some important classes of ML problems such as logistic regression and linear least squares.

Similarly to Proposition 5.1 in [27] we prove that the error of the approximate model  $m_{\mathcal{N}_k}$  can be controlled by the trust region radius.

**Lemma 2.** Suppose that Assumptions 1-2 hold. Then there exists a positive constant  $c_f > 0$  such that for each  $k \in \mathbb{N}$  the step  $d_k$  of ASMOP satisfies

$$|\phi_{\mathcal{N}_k}(x_k + d_k) - m_{\mathcal{N}_k}(d_k)| \leq c_f \delta_k^2.$$

*Proof.* Due to Assumption 1 and Taylor's expansion, for each  $i$  there exists  $\alpha_i^k \in (0, 1)$  such that the following equality holds

$$f_{\mathcal{N}_k^i}^i(x_k + d_k) = f_{\mathcal{N}_k^i}^i(x_k) + \langle \nabla f_{\mathcal{N}_k^i}^i(x_k), d_k \rangle + \frac{1}{2} \langle d_k, \nabla^2 f_{\mathcal{N}_k^i}^i(x_k + \alpha_i^k d_k) d_k \rangle. \quad (21)$$

Furthermore, there holds

$$\begin{aligned} |\phi_{\mathcal{N}_k}(x_k + d_k) - m_{\mathcal{N}_k}(d_k)| &= \left| \max_{i \in \{1, \dots, q\}} f_{\mathcal{N}_k^i}^i(x_k + d_k) - \max_{i \in \{1, \dots, q\}} m_{\mathcal{N}_k^i}(d_k) \right| \\ &\leq \max_{i \in \{1, \dots, q\}} |f_{\mathcal{N}_k^i}^i(x_k + d_k) - m_{\mathcal{N}_k^i}(d_k)| \\ &\leq \max_{i \in \{1, \dots, q\}} \left( \left| \frac{1}{2} \langle d_k, \nabla^2 f_{\mathcal{N}_k^i}^i(x_k + \alpha_i^k d_k) d_k \rangle \right| \right. \\ &\quad \left. + \left| \frac{1}{2} \langle d_k, H_k^i d_k \rangle \right| \right) \\ &\leq \max_{i \in \{1, \dots, q\}} \left( \frac{1}{2} \|d_k\|^2 (c_h + c_b) \right) \leq \frac{1}{2} (c_h + c_b) \delta_k^2 \end{aligned} \quad (22)$$

and the result holds with  $c_f := \frac{1}{2}(c_h + c_b)$ .  $\blacksquare$

**Remark 1.** Notice that if  $M_b^k = \emptyset$ , i.e., if the algorithm is in the FS phase, Lemma 2 implies

$$|\phi(x_k + d_k) - m_k(d_k)| \leq c_f \delta_k^2. \quad (23)$$

The further analysis is conducted by observing the two possible outcomes of the algorithm with respect to sample size behavior (MB and FS) separately. However, at the end we combine all the possible outcomes to form the final result stated in Theorem 4.2. In order to do that, we follow the similar path as in other papers dealing with the considered additional sampling approach. Let us denote by  $\mathcal{D}_k^+$  the subset of all possible outcomes of  $\mathcal{D}_k$  such that  $\rho_{\mathcal{D}_k} \geq \nu$ , i.e.,

$$\mathcal{D}_k^+ = \{\mathcal{D}_k \subset \mathcal{N} \mid \phi_{\mathcal{D}_k}(x_t) \leq \phi_{\mathcal{D}_k}(x_k) + \delta_k \bar{t}_k - \nu \max_{i \in \{1, \dots, q\}} \|\nabla f_{\mathcal{D}_k^i}^i(x_k)\|\}. \quad (24)$$

If  $\mathcal{D}_k \in \mathcal{D}_k^+$  and  $\rho_{\mathcal{N}_k} \geq \eta$  then  $x_{k+1} = x_t$ , otherwise we have  $x_{k+1} = x_k$ . Similarly, we denote the set of outcomes where an increase occurs as

$$\mathcal{D}_k^- = \{\mathcal{D}_k \subset \mathcal{N} \mid \phi_{\mathcal{D}_k}(x_t) > \phi_{\mathcal{D}_k}(x_k) + \delta_k \bar{t}_k - \nu \max_{i \in \{1, \dots, q\}} \|\nabla f_{\mathcal{D}_k^i}^i(x_k)\|\}. \quad (25)$$

Notice that if  $\mathcal{D}_k \in \mathcal{D}_k^-$ , then  $x_{k+1} = x_k$ . Now, we proceed by observing the MB scenario first. The following lemma states that, within this scenario, we have  $\rho_{\mathcal{D}_k} \geq \nu$  for all  $k$  large enough.

**Lemma 3.** If  $M_b \neq \emptyset$  then there exists random, finite iteration  $k_0 \in \mathbb{N}$  such that  $\mathcal{D}_k^- = \emptyset$  for all  $k \geq k_0$ .

*Proof.* Since the sample sizes are nondecreasing, for each  $i \in M_b$  there exist a corresponding  $\bar{N}^i < N$  and  $k_0^i \in \mathbb{N}$  such that  $N_k^i = \bar{N}^i$  for all  $k \geq k_0^i$ . Without loss of generality, let us assume that for all  $j \notin M_b$  there holds  $N_k^j = N$  for all  $k \geq k_0 := \max_{i \in \{1, \dots, q\}} k_0^i$ , i.e., for all  $k \geq k_0$  the subsample sizes reached their upper limit.

Let us assume the contrary, that there exist an infinite subsequence of iterations  $K \subset \mathbb{N}$  such that  $\mathcal{D}_k^- \neq \emptyset$  for all  $k \in K$ . That means that for all  $k \in K$  there exists at least one possible choice of  $\mathcal{D}_k$  such that  $\rho_{\mathcal{D}_k} < \nu$ . Without loss of generality, assume that for all  $k \in K$  we have that  $k \geq k_0$ . Since  $D_k^i \leq N - 1$ , there are finitely many combinations with repetitions for  $\mathcal{D}_k^i$  and thus there are finitely many choices for  $q$ -tuples  $\mathcal{D}_k^1$ . Therefore there exists  $\tilde{p} \in (0, 1)$  such that  $P(\mathcal{D}_k \in \mathcal{D}_k^-) \geq \tilde{p}$ , i.e.,  $P(\mathcal{D}_k \in \mathcal{D}_k^+) \leq 1 - \tilde{p} = p < 1$ . Hence

$$P(\mathcal{D}_k \in \mathcal{D}_k^+, \forall k \in K) \leq \prod_{k \in K} p = 0,$$

i.e., almost surely there exists  $k \geq k_0$ , such that  $\rho_{\mathcal{D}_k} < \nu$ . However, according to Step 2 of the algorithm, the sample size is increased for all  $i \in M_b^k$  in that case, which is a contradiction with the assumption that  $N_k^i = \bar{N}^i$  for all  $i \in M_b$  and  $k \geq k_0$ . This completes the proof.  $\blacksquare$

The following lemma will help us to show that the marginal function tends to zero in the MB scenario. In order to prove the convergence result, we define an auxiliary function  $\Phi_{fix}$

$$\Phi_{fix}(x) := \frac{1}{N} \sum_{j=1}^N \max_{i \in \{1, \dots, q\}} f_j^i(x). \quad (26)$$

The result is as follows.

**Lemma 4.** Suppose that Assumptions 1 holds and  $M_b \neq \emptyset$ . Then

$$\Phi_{fix}(x_t) \leq \Phi_{fix}(x_k) - \nu \omega(x_k) + \delta_k \bar{t}_k$$

holds for all  $k \geq k_0$ , where  $k_0$  is as in Lemma 3.

*Proof.* Lemma 3 implies that we have  $\rho_{\mathcal{D}_k} \geq \nu$ , i.e.,

$$\phi_{\mathcal{D}_k}(x_t) \leq \phi_{\mathcal{D}_k}(x_k) + \delta_k \bar{t}_k - \nu \max_{i \in \{1, \dots, q\}} \|\nabla f_{\mathcal{D}_k^i}^i(x_k)\|,$$

---

<sup>1</sup>More precisely, the number of possible choices for  $\mathcal{D}_k$  is  $S(D_k^i) \leq \bar{S}^i := (2N-2)! / ((N-1)!)^2$  where the upper bound follows from the combinatorics of unordered sampling with replacement. Thus, the number of choices for  $q$ -tuples  $\mathcal{D}_k$  is also finite and bounded by  $\bar{S} = \prod_{i \in M_b} \bar{S}^i$ .

for all  $k \geq k_0$  and for every possible choice of  $\mathcal{D}_k$ . Since the choice of each  $\mathcal{D}_k^i$  is uniform and random with replacements, this further implies<sup>2</sup> that the previous inequality also holds for all the single-element choices of  $\mathcal{D}_k^i$  and all their possible combinations forming  $\mathcal{D}_k$ . Further, observing the combinations of the form  $\mathcal{D}_k = (j, \dots, j)$  for  $j = 1, \dots, N$  we obtain

$$\max_{i \in \{1, \dots, q\}} f_j^i(x_t) \leq \max_{i \in \{1, \dots, q\}} f_j^i(x_k) + \delta_k \bar{t}_k - \nu \max_{i \in \{1, \dots, q\}} \|\nabla f_j^i(x_k)\|.$$

Now, summing over  $j$  and dividing by  $N$  we obtain

$$\Phi_{fix}(x_t) \leq \Phi_{fix}(x_k) + \delta_k \bar{t}_k - \nu \frac{1}{N} \sum_{j=1}^N \max_{i \in \{1, \dots, q\}} \|\nabla f_j^i(x_k)\|. \quad (27)$$

Further, let us observe the marginal function and let us denote by  $d_k^*$  the solution of (3) at iteration  $k$ , i.e.,

$$\omega(x_k) = - \max_{i \in \{1, \dots, q\}} \langle \nabla f^i(x_k), d_k^* \rangle.$$

Then for every  $i \in \{1, \dots, q\}$  there holds

$$-\omega(x_k) = \max_{i \in \{1, \dots, q\}} \langle \nabla f^i(x_k), d_k^* \rangle \geq \langle \nabla f^i(x_k), d_k^* \rangle.$$

Furthermore, by using the Cauchy-Schwartz inequality and the fact that  $\|d_k^*\| \leq 1$  we obtain

$$-\omega(x_k) \geq \langle \nabla f^i(x_k), d_k^* \rangle \geq -\|\nabla f^i(x_k)\| \|d_k^*\| \geq -\|\nabla f^i(x_k)\|.$$

Equivalently,  $\omega(x_k) \leq \|\nabla f^i(x_k)\|$  for every  $i$  and thus we obtain

$$\begin{aligned} \omega(x_k) &\leq \max_{i \in \{1, \dots, q\}} \|\nabla f^i(x_k)\| = \max_{i \in \{1, \dots, q\}} \left\| \frac{1}{N} \sum_{j=1}^N \nabla f_j^i(x_k) \right\| \\ &\leq \max_{i \in \{1, \dots, q\}} \frac{1}{N} \sum_{j=1}^N \|\nabla f_j^i(x_k)\| \leq \frac{1}{N} \sum_{j=1}^N \max_{i \in \{1, \dots, q\}} \|\nabla f_j^i(x_k)\|. \end{aligned} \quad (28)$$

Combining this with (27) we obtain the result. ■

The following result states that in the MB case, eventually all the iterates remain within a random level set of the function  $\Phi_{fix}$ .

**Corollary 4.1.** *Suppose that the assumptions of Lemma 4 hold. Then the following holds for all  $k \in \mathbb{N}$*

$$\Phi_{fix}(x_{k_0+k}) \leq \Phi_{fix}(x_{k_0}) + \delta_{max} \bar{t}.$$

---

<sup>2</sup>Additional sampling is such that it is possible to have  $\mathcal{D}_k^i = \{j, \dots, j\}$  which is in fact equivalent of choosing one-element  $\mathcal{D}_k^i = \{j\}$  due to sample average approximations.

*Proof.* Since  $x_{k+1}$  is either  $x_k$  or  $x_t$ , Lemma 4 and nonnegativity of  $\omega(x_k)$  (Lemma 1, a)) imply that in either case we have  $\Phi_{fix}(x_{k+1}) \leq \Phi_{fix}(x_k) + \delta_k \bar{t}_k$  for every  $k \geq k_0$ . Then, the results follows from summability of  $\bar{t}_k$  (18) and the fact that the sequence of  $\delta_k$  is uniformly bounded by  $\delta_{max}$ . ■

Similar result can be obtained for the FS scenario as well.

**Lemma 5.** Suppose that the Assumptions 1-2 hold. If  $M_b = \emptyset$ , then there exists a finite, random iteration  $k_1$  such that the following holds for all  $k \in \mathbb{N}$

$$\phi(x_{k_1+k}) \leq \phi(x_{k_1}) + \delta_{max} t.$$

*Proof.* Since  $M_b = \emptyset$ , there exists a random, finite iteration  $k_1 \in \mathbb{N}$  such that for all  $k \geq k_1$  the full sample is reached, i.e.,  $N_k^i = N$  for all  $i = 1, \dots, q$ , and thus we have  $\phi_{\mathcal{N}_k}(x_k) = \phi(x_k)$ ,  $m_{\mathcal{N}_k}(d_k) = m_k(d_k)$  and  $\omega_{\mathcal{N}_k}(x_k) = \omega(x_k)$ . Let us observe iterations  $k \geq k_1$  and denote  $\rho_k := \rho_{\mathcal{N}}$ . Then, according to the algorithm, the step is accepted if and only if  $\rho_k \geq \eta$ . So, either  $\phi(x_{k+1}) = \phi(x_k)$  or  $\phi(x_{k+1}) = \phi(x_t)$  and  $\rho_k \geq \eta$ , i.e.,

$$\begin{aligned} \phi(x_{k+1}) &\leq \phi(x_k) + t_k \delta_k + \eta(m_k(d_k) - m_k(0)) \\ &\leq \phi(x_k) + t_k \delta_k - \frac{\eta}{2} \omega(x_k) \min\left\{\delta_k, \frac{\omega(x_k)}{\beta_k}\right\} \\ &\leq \phi(x_k) + t_k \delta_{max}. \end{aligned}$$

Hence the result follows from (14). ■

In order to prove the main result, we assume that the expected value of any local cost function  $f_j^i$  is uniformly bounded. For instance, this is true under the bounded iterates assumption which is common in stochastic framework. More precisely, we assume the following.

**Assumption 3.** There exists a constant  $C > 0$  such that for all  $i = 1, \dots, q$  and  $j \in \mathcal{N}^i$  we have  $\mathbb{E}(|f_j^i(x_{k_0})| \mid MB) \leq C$  and  $\mathbb{E}(|f_j^i(x_{k_1})| \mid FS) \leq C$ .

Notice that Assumption 3 implies that

$$\mathbb{E}(\Phi_{fix}(x_{k_0}) \mid MB) \leq C \quad \text{and} \quad \mathbb{E}(\phi_{fix}(x_{k_1}) \mid FS) \leq C. \quad (29)$$

In the sequel we will show the convergence result for ASMOP algorithm. The analysis is conducted in a similar way as in the proof of Theorem 1 of [13], but adapted to fit the multi-objective framework. For the sake of readability, we observe separately MB and FS case. First we consider the MB scenario and show that  $\liminf_{k \rightarrow \infty} \omega(x_k) = 0$  almost surely.

**Theorem 1.** Suppose that Assumptions 1-3 hold. Then

$$P(\liminf_{k \rightarrow \infty} \omega(x_k) = 0 \mid MB) = 1.$$

*Proof.* Let us consider the MB scenario, i.e., the sample paths such that  $M_b \neq \emptyset$ . Then, Lemma 3 implies that we have  $\rho_{\mathcal{D}_k} \geq \nu$ , for all  $k \geq k_0$  and for every possible choice of  $\mathcal{D}_k$ . Moreover, we know that for each  $i \in M_b$  we have  $N_k^i = \bar{N}^i < N$ , and for each  $i \notin M_b$  we have  $N_k^i = N$  for all  $k \geq k_0$ . Moreover, according to Step 2 of the algorithm, we have

$$\omega_{\mathcal{N}_k}(x_k) \geq \varepsilon h_k^i \geq \varepsilon \frac{1}{N} =: \varepsilon_N > 0$$

for all  $i \in M_b$  and  $k \geq k_0$ . Now, we will show that there exists an infinite subset of iterations at which the trial point is accepted, i.e., that  $\rho_{\mathcal{N}_k} \geq \eta$  occurs infinite number of times.

Suppose the contrary, that there exists  $k_3 \geq k_0$  such that  $\rho_{\mathcal{N}_k} < \eta$  for all  $k \geq k_3$ . This further implies that  $\lim_{k \rightarrow \infty} \delta_k = 0$  due to Step 3 of the algorithm. Moreover, in this scenario, we also have a fixed sample  $\mathcal{N}_k = \mathcal{N}_{k_3}$  for all  $k \geq k_3$ . Furthermore, since  $m_{\mathcal{N}_k}(0) = \phi_{\mathcal{N}_k}(x_k)$ , from Lemma 2 for all  $k \geq k_3$  we have that

$$\begin{aligned} |\rho_{\mathcal{N}_k} - 1| &= \left| \frac{\phi_{\mathcal{N}_k}(x_t) - \phi_{\mathcal{N}_k}(x_k) - t_k \delta_k}{m_{\mathcal{N}_k}(d_k) - m_{\mathcal{N}_k}(0)} - 1 \right| = \left| \frac{\phi_{\mathcal{N}_k}(x_t) - t_k \delta_k - m_{\mathcal{N}_k}(d_k)}{m_{\mathcal{N}_k}(d_k) - m_{\mathcal{N}_k}(0)} \right| \\ &\leq \frac{c_f \delta_k^2 + t_k \delta_k}{\frac{\omega_{\mathcal{N}_k}(x_k)}{2} \min\{\delta_k, \frac{\omega_{\mathcal{N}_k}(x_k)}{\beta_k}\}} \leq \frac{c_f \delta_k^2 + t_k \delta_k}{\frac{\varepsilon_N}{2} \min\{\delta_k, \frac{\varepsilon_N}{c_b}\}}. \end{aligned}$$

Since  $\lim_{k \rightarrow \infty} \delta_k = 0$ , there exists  $k_4 \geq k_3$  such that  $\delta_k < \varepsilon_N / c_b$  for all  $k \geq k_4$  and thus

$$|\rho_{\mathcal{N}_k} - 1| \leq \frac{c_f \delta_k^2 + t_k \delta_k}{\frac{\varepsilon_N \delta_k}{2}} = \frac{2c_f \delta_k + 2t_k}{\varepsilon_N}.$$

Letting  $k \rightarrow \infty$  and using the fact that  $\lim_{k \rightarrow \infty} t_k = 0$  due to (14), we obtain  $\lim_{k \rightarrow \infty} \rho_{\mathcal{N}_k} = 1$ , which is in contradiction with the assumption of  $\rho_{\mathcal{N}_k} < \eta < \frac{3}{4}$  for all  $k \geq k_3$ .

Thus, we have just shown that there exists an infinite subsequence  $K_2 \subset \mathbb{N}$  such that  $\rho_{\mathcal{N}_k} \geq \eta$  for all  $k \in K_2$ . Let  $K_3 = K_2 \cap \{k_0, k_0 + 1, \dots\} := \{k_j\}_{j \in \mathbb{N}}$ . Then, for all  $k \in K_3$  we have  $\rho_{\mathcal{D}_k} \geq \nu$  and  $\rho_{\mathcal{N}_k} \geq \eta$ , and thus  $x_{k+1} = x_t$ . Notice that for all the intermediate iterations, i.e., for all  $k \geq k_0$ ,  $k \notin K_3$  we have  $x_{k+1} = x_k$ . Thus, Lemma 4 implies

$$\Phi_{fix}(x_{k_{j+1}}) = \dots = \Phi_{fix}(x_{k_j+1}) \leq \Phi_{fix}(x_{k_j}) - \nu \omega(x_{k_j}) + \delta_{k_j} \bar{t}_{k_j}$$

and thus for each  $j \in \mathbb{N}$

$$\Phi_{fix}(x_{k_j}) \leq \Phi_{fix}(x_{k_0}) - \nu \sum_{l=0}^{j-1} \omega(x_{k_l}) + \delta_{max} \bar{t}.$$

Applying the conditional expectation  $\mathbb{E}(\cdot | MB)$  and using Assumptions 1 which implies that  $\Phi_{fix}(x_{k_j})$  is bounded from below for any  $j$ , by employing Assumption 3 and letting  $j \rightarrow \infty$  we conclude that

$$\sum_{l=0}^{\infty} \mathbb{E}(\omega(x_{k_l}) | MB) < \infty.$$

Now, for any  $\epsilon$ , from Markov's inequality we obtain

$$\sum_{l=0}^{\infty} P(\omega(x_{k_l}) \geq \epsilon | MB) \leq \frac{1}{\epsilon} \sum_{l=0}^{\infty} \mathbb{E}(\omega(x_{k_l}) | MB) < \infty.$$

Finally, Borel-Cantelli Lemma implies that  $\lim_{l \rightarrow \infty} \omega(x_{k_l}) = 0$  which completes the proof.  $\blacksquare$

Next, we show the same result for the FS scenario.

**Theorem 2.** Suppose that Assumptions 1-3 hold. Then

$$P(\liminf_{k \rightarrow \infty} \omega(x_k) = 0 | FS) = 1.$$

*Proof.* Let us consider the FS scenario, i.e., the sample paths such that  $M_b = \emptyset$ . Then, as in the proof of Lemma 5, for all  $k \geq k_1$  we have  $N_k^i = N$  for all  $i = 1, \dots, q$ , and thus  $\phi_{N_k}(x_k) = \phi(x_k)$ ,  $m_{N_k}(d_k) = m_k(d_k)$ ,  $\omega_{N_k}(x_k) = \omega(x_k)$  and  $\rho_k := \rho_N$ .

Let us suppose the the statement of this theorem is not true, i.e., that there exists  $\epsilon > 0$  and  $k_2 \geq k_1$  such that  $\omega(x_k) > \epsilon$  for all  $k \geq k_2$ . Since (14) implies that  $\lim_{k \rightarrow \infty} t_k = 0$ , without loss of generality, assume that  $t_k < c_f$  for all  $k \geq k_2$ . Then it can be shown that the sequence of  $\delta_k$  is uniformly bounded away from zero. Indeed, if at any iteration  $k \geq k_2$  the value of  $\delta_k$  falls below  $\hat{\delta} := \epsilon / (20 \max\{1, c_f, c_b\})$ , then Lemma 2 implies

$$\begin{aligned} |\rho_k - 1| &= \left| \frac{\phi(x_k) - m_k(d_k) - t_k \delta_k}{m_k(d_k) - m_k(0)} \right| \leq \frac{c_f \delta_k^2 + t_k \delta_k}{\frac{\omega(x_k)}{2} \min\{\delta_k, \frac{\omega(x_k)}{\beta_k}\}} \\ &\leq \frac{c_f \delta_k^2 + t_k \delta_k}{\frac{\epsilon}{2} \min\{\delta_k, \frac{\epsilon}{c_b}\}} \leq \frac{c_f \delta_k^2 + t_k \delta_k}{\frac{\epsilon}{2} \delta_k} < \frac{c_f \hat{\delta} + c_f \hat{\delta}}{\frac{\epsilon}{2}} < \frac{1}{4} \end{aligned}$$

which further implies that  $\rho_k > \frac{3}{4} > \eta$ , and, according to the algorithm, the radius is increased, i.e.,  $\delta_{k+1} > \delta_k$ . Therefore, there exists  $\tilde{\delta} > 0$ , such that  $\delta_k > \tilde{\delta}$ , for all  $k \geq k_2$ .

On the other hand, the existence of  $k_3$  such that  $\rho_k < \eta$  for every  $k \geq k_3$  would imply  $\lim_{k \rightarrow \infty} \delta_k = 0$  due to Step 4 of the algorithm, which is in contradiction with  $\delta_k > \tilde{\delta}$ , for all  $k \geq k_2$ . Thus, we conclude that there

must exist an infinite number of iterations  $K_1 \subset \mathbb{N}$  such that for all  $k \in K_1$  there holds  $k \geq k_2$  and  $\rho_k \geq \eta$ . Therefore, for all  $k \in K_1$  we have

$$\begin{aligned} \phi(x_{k+1}) &\leq \phi(x_k) + \delta_k t_k + \eta(m_k(d_k) - m_k(0)) \\ &\leq \phi(x_k) + \delta_k t_k - \eta \frac{\omega(x_k)}{2} \min\{\delta_k, \frac{\omega(x_k)}{\beta_k}\} \\ &\leq \phi(x_k) + \delta_k t_k - \eta \frac{\varepsilon}{2} \min\{\tilde{\delta}, \frac{\varepsilon}{c_b}\} \\ &=: \phi(x_k) + \delta_k t_k - \hat{c}. \end{aligned}$$

Again, without loss of generality, we can assume that for all  $k \in K_1$  there holds  $\delta_k t_k \leq \hat{c}/2$  and thus

$$\phi(x_{k+1}) \leq \phi(x_k) - \frac{\hat{c}}{2}, \quad k \in K_1.$$

Furthermore, by denoting  $K_1 = \{k_j\}_{j \in \mathbb{N}}$  and using the fact that for all  $k \geq k_2$  such that  $k \notin K_1$  the trial point is rejected and thus  $\phi(x_{k+1}) = \phi(x_k)$ , we conclude that for all  $j \in \mathbb{N}$

$$\phi(x_{k_{j+1}}) = \dots = \phi(x_{k_j+1}) \leq \phi(x_{k_j}) - \frac{\hat{c}}{2}.$$

Applying the conditional expectation and using Assumption 3 we obtain that for every  $j \in \mathbb{N}$

$$\mathbb{E}(\phi(x_{k_j}) \mid FS) \leq C - j \frac{\hat{c}}{2}$$

and letting  $j \rightarrow \infty$  we obtain  $\lim_{j \rightarrow \infty} \mathbb{E}(\phi(x_{k_j}) \mid FS) = -\infty$ . This is in contradiction with Assumption 1 which implies that the function  $\phi$  is bounded from below. This completes the proof.  $\blacksquare$

Finally, we obtain the following result as a direct consequence of the previous two theorems and Lemma 1.

**Corollary 4.2.** *Suppose that Assumptions 1-3 hold. Then the sequence of iterates  $\{x_k\}_{k \in \mathbb{N}}$  generated by the ASMOP algorithm satisfies*

$$\liminf_{k \rightarrow \infty} \omega(x_k) = 0 \quad a.s.$$

*Moreover, if the sequence of iterates is bounded, then a.s. there exists an accumulation point of the sequence  $\{x_k\}_{k \in \mathbb{N}}$  which is a Pareto critical point for problem (1).*

## 5 Numerical results

In this section we showcase numerical results obtained on machine learning problems. The proposed algorithm - ASMOP is compared to the state-of-the-art stochastic multi-gradient method SMG [20] for multi-objective problems. We also compare ASMOP to SMOP [17] which also uses sample average approximations, but different sample size guidance. The comparison is made through FEV (number of function evaluations) and CPU time. The first measure is relevant for problems where accessing the data represents a dominant cost and it also serves as a proxy for computational cost. The other measure is relevant in applications such as portfolio optimization in finance, where the approximate solution needs to be obtained promptly. It is, however, sensitive to implementation issues which may not be optimal for all the considered methods. Nevertheless, the results reveal potentials of ASMOP considering both measures.

We tested the relevant methods on different types of problems. Section 5.1 covers convex problems where the objectives are constructed through regularized logistic regression models. In Section 5.2 we present the results obtained on different types of objectives - one objective is modeled by regularized nonconvex loss in 2-layer Neural Networks, while the other one represents a least squares problem coming from, e.g., linear regression. Additionally, within Section 5.3 we compare different parameter configurations of ASMOP and demonstrate algorithm's behavior under different sample size increments. In all sections, since the gradients and Hessians reuse intermediate quantities computed during the loss evaluation (e.g.,  $x^T a_j$ ), they can be obtained with a negligible additional computational cost. Therefore, one FEV accounts for the joint evaluation of the function, gradient, and Hessian of a single function  $f_j^i$ .

### 5.1 Logistic regression

The first set of experiments consists of minimizing the regularized logistic regression loss function with the CIFAR10, MNIST and Fashion MNIST dataset. CIFAR10 is a dataset for an image classification problem, and it consists of  $N = 5 \times 10^4$  RGB images of  $32 \times 32$  pixels in 3 hues, which are in 10 categories, hence the dimension of the problem is  $n = 32 \times 32 \times 3 = 3072$ . We create a model which differentiates category 0 (airplane) from 1 (car), and also category 2 (bird) from 3 (cat) at the same time. Assuming  $\mathcal{N}$  is the set of indices of the training dataset, we split the dataset into two subsets by creating two index subgroups  $\mathcal{N}^1$  and  $\mathcal{N}^2$  such that  $\mathcal{N}^1$  are indices of the samples which are in categories 0 and 1, and  $\mathcal{N}^2$  are indices of the samples in categories 2 and 3. The second dataset we used was the MNIST dataset which consists of  $N = 7 \times 10^4$  samples of gray-scale images of handwritten digits with  $32 \times 32$  pixels, hence the dimension is  $n = 1024$ . Once again,

we created two datasets from MNIST, the first containing samples with labels 0 and 8, and the second with labels 1 and 4. This way the model differentiates digits 0 or 8, and digits 1 and 4 at the same time, similarly as with CIFAR10. We made both subgroups contain the same amount of elements  $N = 10^4$ . The third dataset we used was the Fashion MNIST dataset which consists of  $N = 7 \times 10^4$  samples of gray-scale images of clothing items with  $32 \times 32$  pixels, hence the dimension is  $n = 1024$ . Once again, we created two datasets from Fashion MNIST, the first containing samples with labels 0 and 1, corresponding to T-shirt/top and trouser, and the second with labels 2 and 3, corresponding to pullover and dress. This way the model differentiates T-shirt/top or trouser, and pullover or dress at the same time, similarly as with CIFAR10 and MNIST. We made both subgroups contain the same amount of elements  $N = 10^4$ . Finally, we considered the MNIST-Fairness dataset, which is derived from the MNIST dataset. As before, the original dataset consists of  $N = 7 \times 10^4$  gray-scale images of handwritten digits with  $32 \times 32$  pixels, hence the dimension is  $n = 1024$ . From this dataset we selected only the samples with labels 1 and 4, corresponding to the handwritten digits 1 and 4.

In order to introduce a sensitive attribute, we considered the pixel at position 162 and split the samples according to whether the pixel value was smaller or larger than its average value over the dataset. This procedure generates two subgroups of data, which can be interpreted as two sensitive groups. As mentioned, we are minimizing a regularized logistic regression loss function

$$\min_{x \in \mathbb{R}^n} f(x) := (f^1(x), f^2(x)), \quad (30)$$

where the function components are defined as follows:

$$f^i(x) = \frac{1}{N} \sum_{j \in \mathcal{N}^i} \log(1 + e^{(-y_j(x^T a_j))}) + \frac{\lambda_i}{2} \|\hat{x}\|^2, i = 1, 2. \quad (31)$$

Here,  $x \in \mathbb{R}^n$  represents model coefficients we are trying to find,  $\hat{x}$  coefficient vector without the intercept,  $a_j$  the feature vector and  $y_j$  the relevant label.

There are several factors and parameter choices which influence the behavior of the algorithm. For this experiment, we set the initial subsampling size  $N_0^i = 0.01N$ , and we update the size at Step 2 when needed by a small amount,  $\Delta N_k^i = 0.02N$ . For the nonmonotonicity parameters we set  $t_k = \frac{1}{(k+1)^{1.51}}$ , and  $\bar{t}_k = \frac{100}{(k+1)^{1.51}}$ , which satisfy (14) and (18). Since the power of the denominator is slightly larger than 1, the algorithm will slowly and gradually decrease the tolerance towards the rise of the function value. Both additional sampling sizes  $D_k^1$  and  $D_k^2$  are set to 2 for all iterations in order to keep the additional sampling computationally cheap. We compare algorithms' true marginal function values  $\omega(x_k)$  as a measure of stationarity for multi-objective problems. We calculate  $\omega(x_k)$  at each iteration and plot

it against the FEV or CPU time. For all the considered methods, we perform 5 runs with the same parameters and report the plots of the averaged values. In the plots of  $\omega(x_k)$ , a shaded region is shown to represent the Standard Deviation.

The following Figures 1, 2, 3 and 4 compare the three mentioned algorithms for the fixed budget of  $8 \cdot 10^6$  function evaluation and 80 seconds for CIFAR10 dataset,  $10^6$  and 3 seconds for MNIST dataset,  $2 \cdot 10^6$  and 6 seconds for Fashion MNIST dataset and  $10^5$  and 0.3 seconds for MNIST-Fairness dataset. We have also included the subsampling sizes of SMOP and ASMOP for both function components in all figures. It is evident that ASMOP uses small amount of information to achieve large function reduction. We have noticed that if we set 1% of samples as a starting size, and increase the size of both subsamples by 2% of the respective maximum sample size, the subsampling sizes update similarly for both criteria  $f^1$  and  $f^2$ .

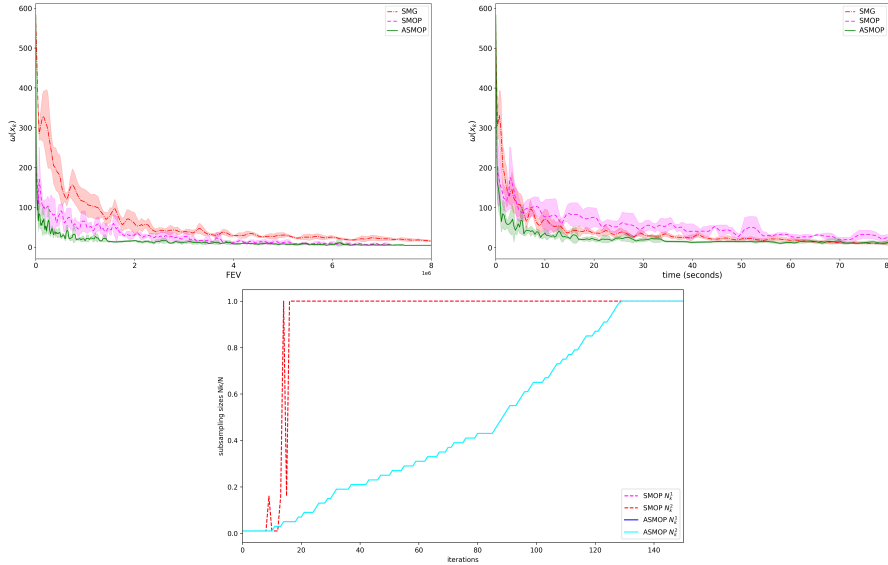


Figure 1: CIFAR10 dataset, problem (31),  $N = 10^4, n = 3072$ . First row: optimality measure against function evaluations (left) and optimality measure against time in second (left). Second row: sample sizes behavior. Parameters:  $x_0 = (0.1, 0.1, \dots, 0.1)$ ,  $\delta_0 = 1$ ,  $\delta_{max} = 8$ ,  $\gamma_1 = 0.5$ ,  $\gamma_2 = 2$ ,  $\nu = 10^{-4}$ ,  $\eta = 0.25$ ,  $\varepsilon = 10^{-9}$ .

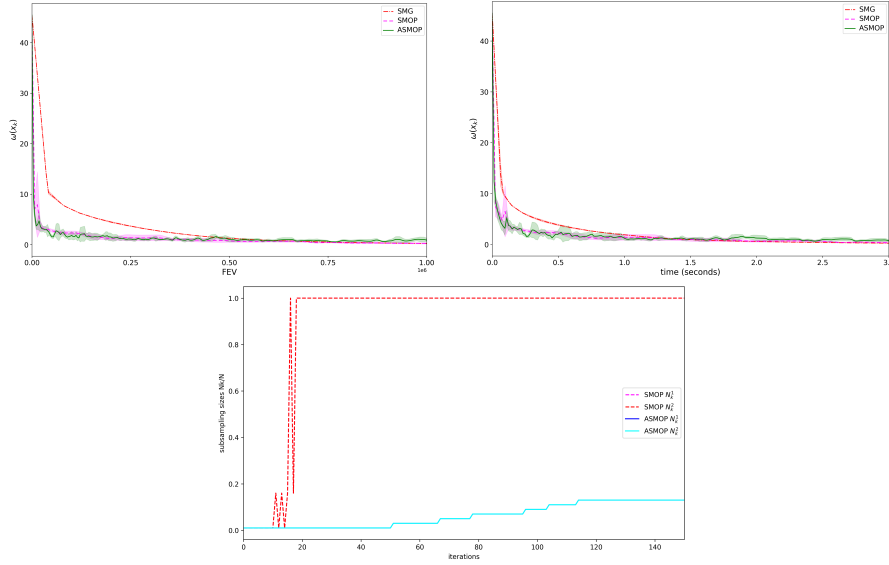


Figure 2: MNIST dataset, problem (31),  $N = 10^4$ ,  $n = 1024$ . First row: optimality measure against function evaluations (left) and optimality measure against time in second (left). Second row: sample sizes behavior. Parameters:  $x_0 = (0.1, 0.1, \dots, 0.1)$ ,  $\delta_0 = 1$ ,  $\delta_{max} = 8$ ,  $\gamma_1 = 0.5$ ,  $\gamma_2 = 2$ ,  $\nu = 10^{-4}$ ,  $\eta = 0.25$ ,  $\varepsilon = 10^{-4}$ .

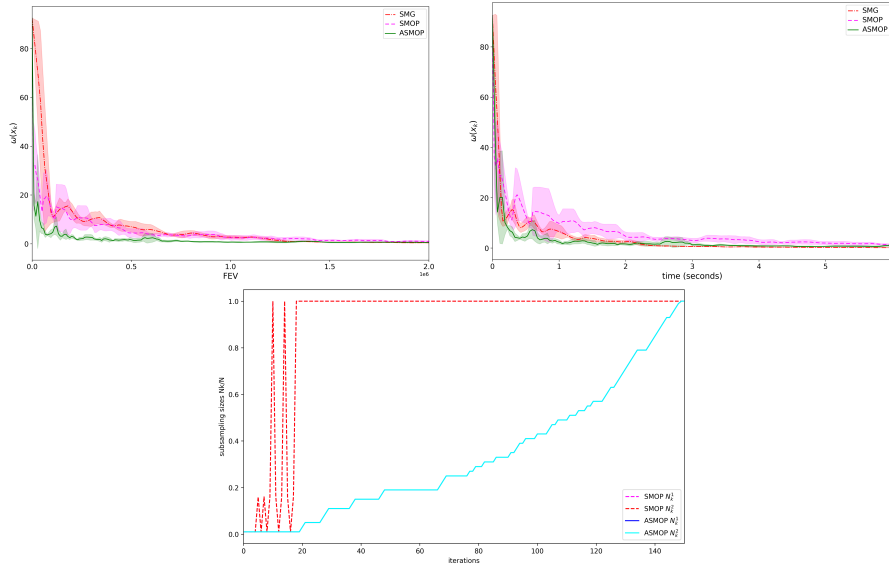


Figure 3: Fashion MNIST dataset, problem (31),  $N = 10^4$ ,  $n = 1024$ . First row: optimality measure against function evaluations (left) and optimality measure against time in second (left). Second row: sample sizes behavior. Parameters:  $x_0 = (0.1, 0.1, \dots, 0.1)$ ,  $\delta_0 = 1$ ,  $\delta_{max} = 8$ ,  $\gamma_1 = 0.5$ ,  $\gamma_2 = 2$ ,  $\nu = 10^{-4}$ ,  $\eta = 0.25$ ,  $\varepsilon = 10^{-4}$ .

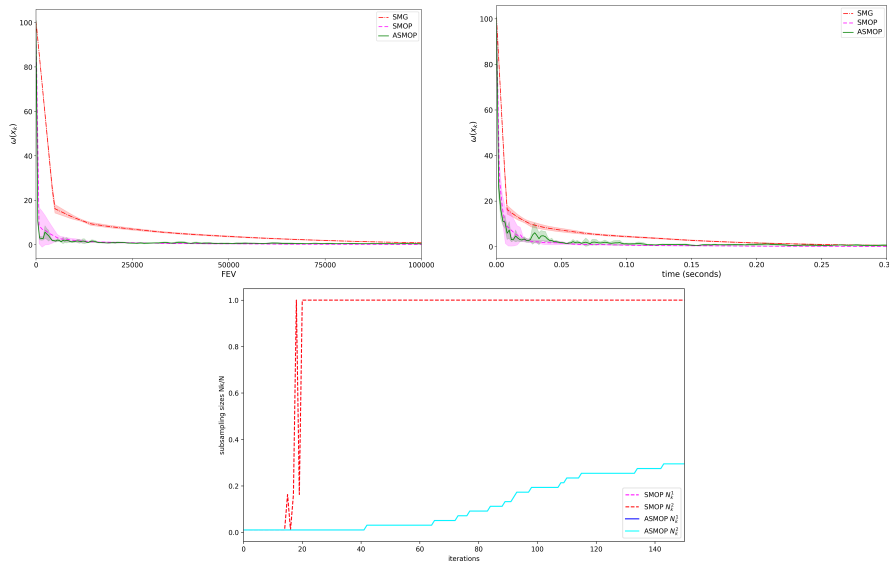


Figure 4: MNIST-Fairness dataset, problem (31),  $N = 10^4$ ,  $n = 1024$ . First row: optimality measure against function evaluations (left) and optimality measure against time in second (right). Second row: sample sizes behavior. Parameters:  $x_0 = (0.1, 0.1, \dots, 0.1)$ ,  $\delta_0 = 1$ ,  $\delta_{max} = 8$ ,  $\gamma_1 = 0.5$ ,  $\gamma_2 = 2$ ,  $\nu = 10^{-4}$ ,  $\eta = 0.25$ ,  $\varepsilon = 10^{-4}$ .

## 5.2 Regularized Nonconvex loss in 2-layer Neural Networks and Least squares

We have also tested how the ASMOP behaves when the criteria are two completely different loss functions. Once again we have used CIFAR10, MNIST, Fashion MNIST and MNIST-Fairness dataset for an image classification problem. The problem we are solving is (30), however this time the component functions are

$$f^1(x) = \frac{1}{N} \sum_{j \in \mathcal{N}^1} \left( 1 - \frac{1}{1 + e^{(-y_j(x^T a_j))}} \right)^2 + \frac{\lambda_1}{2} \|\hat{x}\|^2$$

and

$$f^2(x) = \frac{1}{N} \sum_{j \in \mathcal{N}^2} \frac{1}{2} (x^T a_j - y_j)^2 \quad (32)$$

where  $N$  is the size of the respective sample groups,  $x \in \mathbb{R}^n$  is the vector of model coefficients,  $\hat{x}$  coefficient vector without the intercept,  $a_j$  the attribute vector of the sample and  $y_j$  its respective label. By minimizing this loss function, we get coefficients that are adjusted for both machine learning models. Specifically, for CIFAR10 it will use a regularized Nonconvex loss in 2-layer Neural Networks to differentiate images of cars and planes, and weighted least squares method to differentiate birds from cats, and analogously for the other three datasets considered. In the similar manner, we

set the initial subsampling sizes  $N_0^i = 0.01N$ , and the step size update to  $\Delta N_k^i = 0.02N$ . The predetermined nonmonotonicity sequences were set to  $t_k = \frac{1}{(k+1)^{1.51}}$  and  $\bar{t}_k = \frac{100}{(k+1)^{1.51}}$  as in the previous experiment. The following figures show  $\omega(x_k)$  values in terms of number of function evaluations for a fixed budget of  $7 \cdot 10^6$  for CIFAR10,  $10^6$  for MNIST,  $10^7$  for Fashion MNIST and  $10^5$  for MNIST-Fairness dataset. We also plot  $\omega(x_k)$  against the execution time for a fixed budget of 100 seconds for CIFAR10, 5 seconds for MNIST, 25 seconds for Fashion MNIST and 2 seconds for MNIST-Fairness. In all Figures 5, 6, 7 and 8 it can be seen that for the given budget ASMOP shows efficiency and a large decrease in  $\omega(x_k)$  value for a small cost. Also in this case, five runs are performed and the reported curves correspond to the average results for each method. In the plots of  $\omega(x_k)$ , the shaded region represents the Standard Deviation.

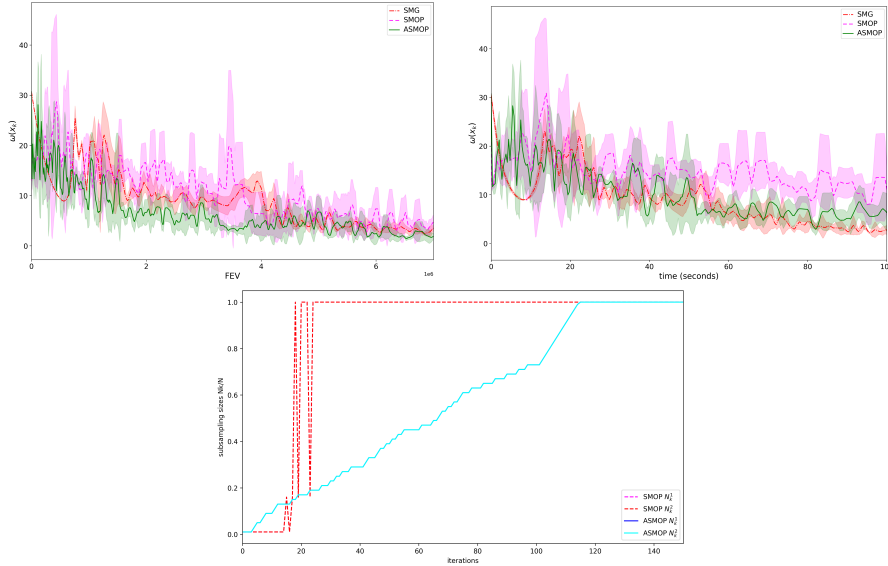


Figure 5: CIFAR10 dataset, problem (32),  $N = 10^4$ ,  $n = 3072$ . First row: optimality measure against function evaluations (left) and optimality measure against time in second (left). Second row: sample sizes behavior. Parameters:  $x_0 = (0.1, 0.1, \dots, 0.1)$ ,  $\delta_0 = 1$ ,  $\delta_{max} = 8$ ,  $\gamma_1 = 0.5$ ,  $\gamma_2 = 2$ ,  $\nu = 10^{-5}$ ,  $\eta = 0.25$ ,  $\varepsilon = 10^{-5}$ .

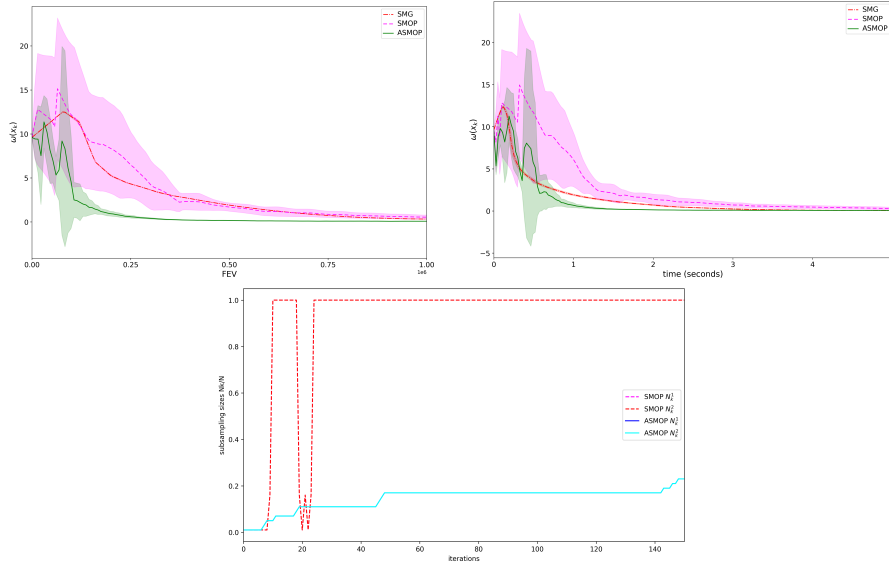


Figure 6: MNIST dataset, problem (32),  $N = 10^4$ ,  $n = 1024$ . First row: optimality measure against function evaluations (left) and optimality measure against time in second (left). Second row: sample sizes behavior. Parameters:  $x_0 = (0.1, 0.1, \dots, 0.1)$ ,  $\delta_0 = 1$ ,  $\delta_{max} = 8$ ,  $\gamma_1 = 0.5$ ,  $\gamma_2 = 2$ ,  $\nu = 10^{-5}$ ,  $\eta = 0.05$ ,  $\varepsilon = 10^{-5}$ .

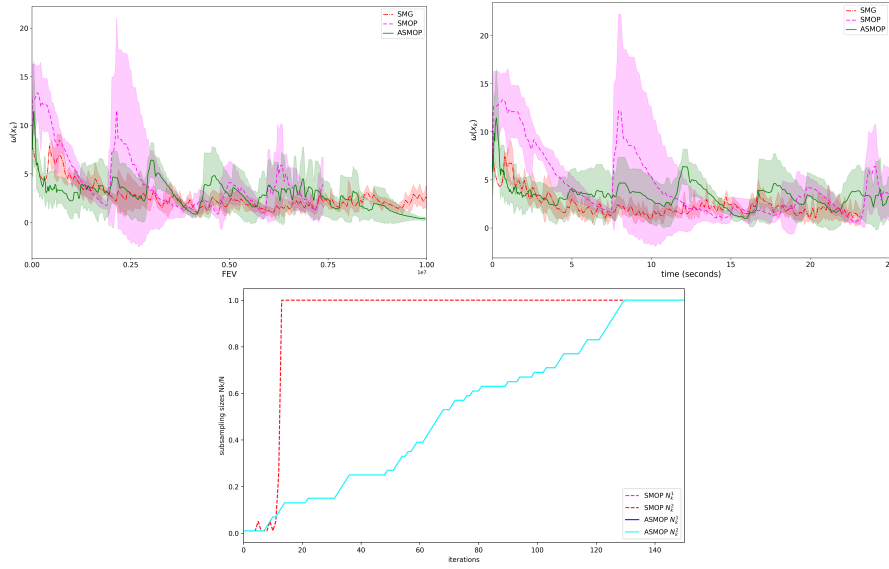


Figure 7: Fashion MNIST dataset, problem (32),  $N = 10^4$ ,  $n = 1024$ . First row: optimality measure against function evaluations (left) and optimality measure against time in second (left). Second row: sample sizes behavior. Parameters:  $x_0 = (0.1, 0.1, \dots, 0.1)$ ,  $\delta_0 = 1$ ,  $\delta_{max} = 8$ ,  $\gamma_1 = 0.6$ ,  $\gamma_2 = 1.5$ ,  $\nu = 10^{-5}$ ,  $\eta = 0.01$ ,  $\varepsilon = 10^{-4}$ .

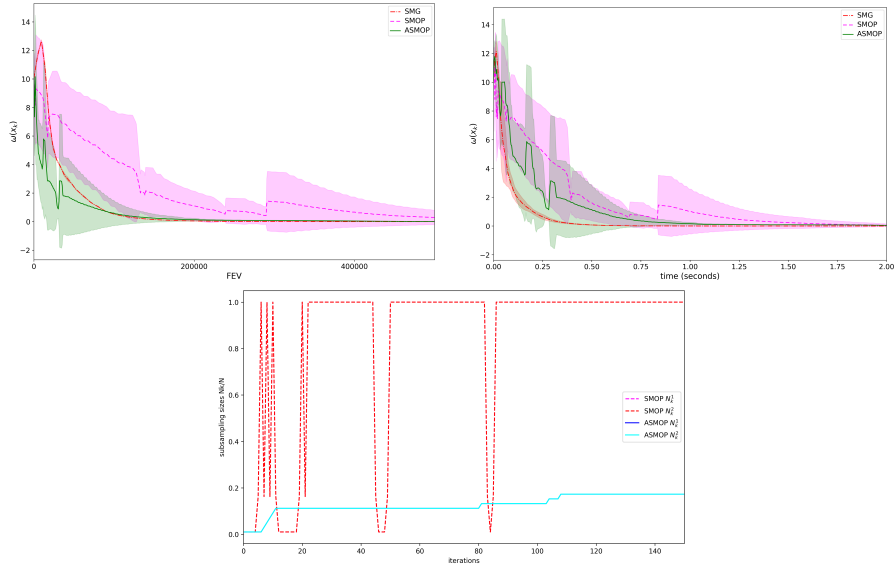


Figure 8: MNIST-Fairness dataset, problem (32),  $N = 10^4$ ,  $n = 1024$ . First row: optimality measure against function evaluations (left) and optimality measure against time in second (left). Second row: sample sizes behavior. Parameters:  $x_0 = (0.1, 0.1, \dots, 0.1)$ ,  $\delta_0 = 1$ ,  $\delta_{max} = 8$ ,  $\gamma_1 = 0.5$ ,  $\gamma_2 = 2$ ,  $\nu = 10^{-5}$ ,  $\eta = 0.05$ ,  $\varepsilon = 10^{-5}$ .

### 5.3 Nonmonotonicity parameters and increasing rule

In the previous experiments, we set parameters  $t_k$  as  $\frac{1}{(k+1)^{1.51}}$  and  $\bar{t}_k$  as  $\frac{100}{(k+1)^{1.51}}$ . By adjusting these settings it is possible to increase or decrease the tolerance of the nonmonotonicity, which leads to different algorithm behavior. We set

$$\bar{t}_k = \frac{C_2}{(k+1)^{1.51}}$$

and tested three different scenarios ( $C_2 \in \{1, 100, 10000\}$ ) in order to see how the relaxation of the condition  $\rho_{\mathcal{D}_k} > \nu$  impacts the performance. The following table shows the chosen settings of the compared algorithms for MNIST dataset, whereas the rest of the parameters were set as in the second experiment.

(MNIST)	$C_2$
ASMOP_1	10000
ASMOP_2	1
ASMOP_3	100

Table 1: MNIST dataset. Different nonmonotonicity settings for ASMOP versions.

We compared these three algorithms similarly as in previous experiments, by criticality measure  $\omega(x_k)$  in terms of function evaluations and time in seconds. The problem being solved is (31). Like the previous cases, five runs are performed and the reported curves correspond to the average results for each method. In the plots of  $\omega(x_k)$ , the shaded region represents the Standard Deviation.

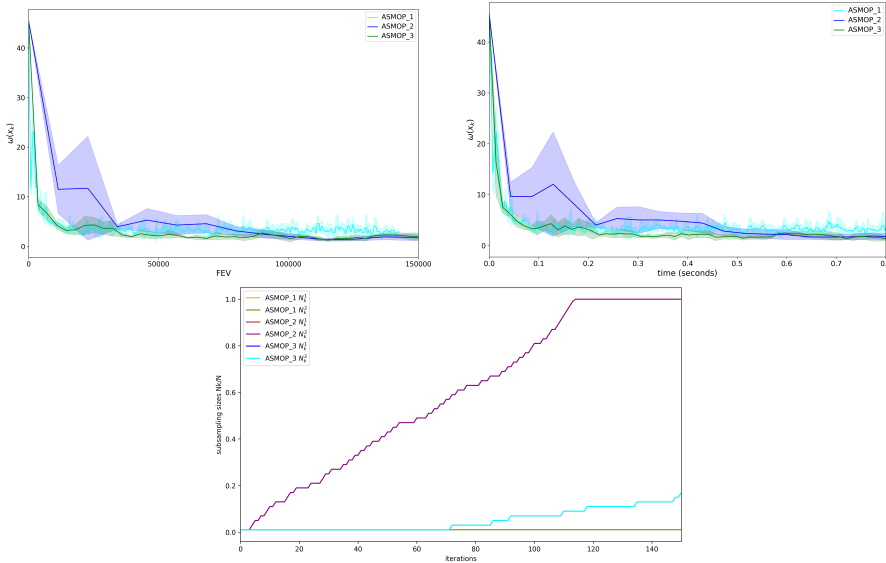


Figure 9: MNIST dataset, problem (31) different settings Table 1,  $N = 10^4$ ,  $n = 1024$ . Optimality measure against computational cost. Parameters:  $x_0 = (0.1, 0.1, \dots, 0.1)$ ,  $\delta_0 = 1$ ,  $\delta_{max} = 8$ ,  $\gamma_1 = 0.5$ ,  $\gamma_2 = 2$ ,  $\nu = 10^{-4}$ ,  $\eta = 0.25$ ,  $\varepsilon = 10^{-4}$ .

It is noticeable that the subsampling sizes are increased less frequently for the versions that have a more relaxed coefficient  $\rho_{\mathcal{D}_k}$ , which means that the higher tolerance leads to the condition  $\rho_{\mathcal{D}_k} > \nu$  being satisfied more often in Step 2 of the algorithm.

We now investigate the influence of different increasing rules for the subsampling sizes. In the previous experiments, the subsampling size was updated like  $\Delta N_k^i = 0.02N$ .

In order to analyze how the growth strategy of the subsampling size affects the behavior of the method, we consider three different increasing rules. The third one corresponds to the rule used in the previous experiments, while the other two introduce alternative strategies for enlarging the sample size during the iterations.

More precisely, we compare the following three variants of the algorithm, each associated with a different increasing rule for the subsampling sizes for MNIST dataset.

(MNIST)	Increasing rule
ASMOP_+1	$\Delta N_k^i = 1$ and $C_2 = 1$
ASMOP_2%	$\Delta N_k^i = 0.02N$ and $C_2 = 1$
ASMOP_2%_RELAX	$\Delta N_k^i = 0.02N$ and $C_2 = 100$

Table 2: MNIST dataset. Different increasing rules for the subsampling size.

As in the previous experiments, the algorithms are compared using the criticality measure  $\omega(x_k)$  with respect to the number of function evaluations and the execution time. The problem being solved is again (31), and all the parameters are kept the same as in the previous experiment unless otherwise specified.

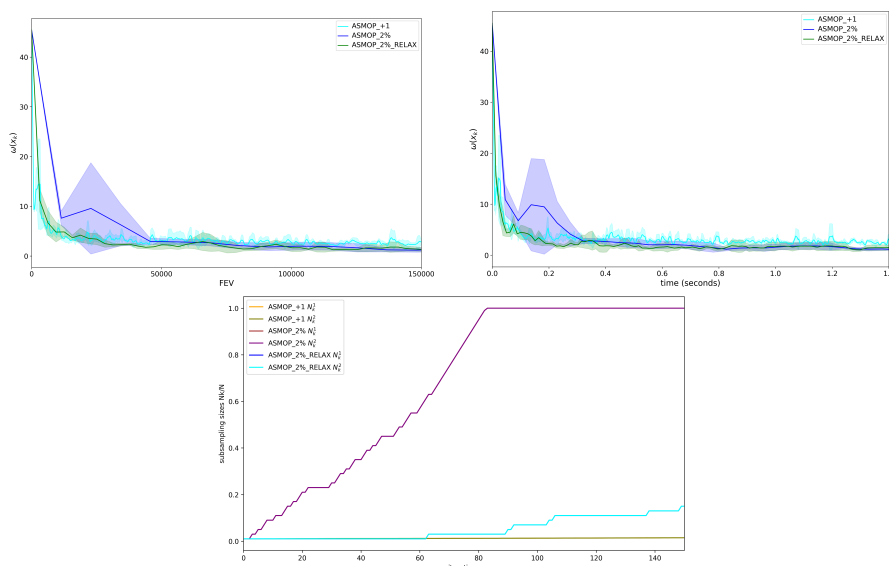


Figure 10: MNIST dataset, problem (31) different settings Table 2,  $N = 10^4$ ,  $n = 1024$ . Optimality measure against computational cost. Parameters:  $x_0 = (0.1, 0.1, \dots, 0.1)$ ,  $\delta_0 = 1$ ,  $\delta_{max} = 8$ ,  $\gamma_1 = 0.5$ ,  $\gamma_2 = 2$ ,  $\nu = 10^{-4}$ ,  $\eta = 0.25$ ,  $\varepsilon = 10^{-4}$ .

It can be observed that the different increasing rules lead to significantly different growth patterns of the subsampling sizes. In particular, the rule used in ASMOP\_2% increases the sample size very aggressively, quickly reaching the full dataset. On the other hand, ASMOP\_+1 enlarges the sample very slowly.

The strategy adopted in ASMOP\_2%\_RELAX provides a more balanced behavior, allowing the algorithm to work with smaller subsamples for a longer portion of the iterations while still progressively increasing the accuracy of the function evaluations. As a consequence, ASMOP\_2%\_RELAX achieves a favorable trade-off between computational cost and convergence

speed, which motivated its selection in the rest of the experiments. The choice of optimal hyper-parameters in an important question and it will be addressed in the future work.

## 6 Conclusion

Stochastic trust region algorithm for unconstrained multi-objective finite sum problems has been proposed. The method is featured by adaptive sample strategy which, depending on the problem, yields a mini-batch or increasing sample size scheduling. The sample size is governed by the additional sampling approach, thus the ASMOP method can be viewed as a generalization of method proposed in [13] for single-objective problems. The adaptation to multi-objective setup required nontrivial modifications, including the additional sampling criterion. Theoretical analysis also required nontrivial adjustments combining additional sampling and multi-objective analysis. We proved almost sure convergence towards Pareto critical points under assumptions that are standard for multi-objective and additional sampling framework, covering a large class of machine learning problems. Numerical study conducted on different machine learning models, covering both convex and nonconvex functions, showed the potential of the proposed method and its competitiveness with the relevant existing methods. We also presented a short analysis of different parameters influencing the sample size dynamics which revealed a direction to follow in some future research.

## Acknowledgments

N. Krklec Jerinkić and L. Rutešić were supported by the Science Fund of the Republic of Serbia, GRANT No 7359, Project LASCADO. The work of I. Trombini was supported by “Gruppo Nazionale per il Calcolo Scientifico (GNCS-INdAM)” (Progetti 2026).

## Availability of Data and Materials

The datasets analyzed during the current study are available in links given in the paper.

## Conflict of interest

The authors have no relevant financial or non-financial interests to disclose.

## References

- [1] BELLAVIA, S., KREJIĆ, N. & MORINI, B. (2020) Inexact restoration with subsampled trust region methods for finite-sum minimization. *Comput Optim Appl* 76, 701–736.
- [2] BERAHAS A. S., BOLLAPRAGADA R. & NOCEDAL J. (2020) An Investigation of Newton-Sketch and Subsampled Newton Methods, *Optimization Methods and Software*, 35(4), 661–680.
- [3] BOLLAPRAGADA, R., BYRD, R. & NOCEDAL, J. (2019) Exact and Inexact Subsampled Newton Methods for Optimization, *IMA Journal of Numerical Analysis*, 39(20), 545–578.
- [4] BOTTOU, L., CURTIS F.E., NOCEDAL, J. (2018) Optimization Methods for LargeScale Machine Learning, *SIAM Review*, 60(2), 223–311.
- [5] BYRD, R.H., HANSEN, S.L., NOCEDAL, J. & SINGER, Y. (2016) A Stochastic QuasiNewton Method for Large-Scale Optimization, *SIAM Journal on Optimization*, 26(2), 1008–1021
- [6] BYRD, R.H., CHIN, G.M., NOCEDAL, J. & WU, Y. (2012) Sample size selection in optimization methods for machine learning, *Mathematical Programming*, 134(1), 127–155.
- [7] CAO, L., BERAHAS, A.S. & SCHEINBERG, K. (2024) First- and second-order high probability complexity bounds for trust region methods with noisy oracles. *Math. Program*, 207, 55–106
- [8] CHEN, R., MENICKELLY, M. & SCHEINBERG, K. (2018) Stochastic optimization using a trust region method and random models, *Math. Program.*, 169, 447–487.
- [9] CUSTODIO, A.L., MADEIRA, J.A., VAZ, A.I.F. & VICENTE, L. N. (2011) Direct multisearch for multiobjective optimization. *SIAM J. Optim*, 21, 1109–1140.
- [10] FLIEGE, J. & SVAITER, B.F. (2000) Steepest Descent Methods for Multicriteria Optimization, *Mathematical Methods of Operations Research*, 51, 479–494.
- [11] FUKUDA, E. H. & DRUMMOND, L. M. G. (2014) A survey on multi-objective descent methods. *Pesq. Oper*, 34 (3).
- [12] IUSEM, A.N., JOFRÉ, A., OLIVEIRA R.I. & THOMPSON P. (2019) Variance-Based Extragradient Methods with Line Search for Stochastic Variational Inequalities *SIAM Journal on Optimization*, 29, 175 - 206

- [13] KREJIĆ, N., KRKLEC JERINKIĆ, N., MARTÍNEZ, A. & YOUSEFI, M. (2024) A non-monotone trust region method with noisy oracles and additional sampling. *Comput Optim Appl*, 89, 247–278.
- [14] KREJIĆ, N., & KRKLEC, N., (2013) Line search methods with variable sample size for unconstrained optimization, *Journal of Computational and Applied Mathematics* 245, pp. 213-231.
- [15] KREJIĆ, N., & KRKLEC JERINKIĆ N., (2019) Spectral projected gradient method for stochastic optimization, *Journal of Global Optimization* 73,1, pp. 59-81
- [16] KREJIĆ, N. & KRKLEC JERINKIĆ, N. (2015) Nonmonotone line search methods with variable sample size, *Numerical Algorithms*, 68(4), 711-739.
- [17] KREJIĆ, N., KRKLEC JERINKIĆ, N. & RUTEŠIĆ, L. (2025) SMOP: Stochastic trust region method for multi-objective problems <https://arxiv.org/abs/2501.06350>
- [18] KREJIĆ, N., LUŽANIN, Z., OVCIN, Z., & STOJKOVSKA, I. (2015). Descent direction method with line search for unconstrained optimization in noisy environment. *Optimization Methods and Software*, 30(6), 1164–1184.
- [19] KRKLEC JERINKIĆ, N., RUGGIERO, V. & TROMBINI, I. (2025) Spectral stochastic gradient method with additional sampling for finite and infinite sums. *Comput Optim Appl* 91, 717–758
- [20] LIU, S. & VICENTE, L.N. (2024) The stochastic multi-gradient algorithm for multi-objective optimization and its application to supervised machine learning, *Ann Oper Res*, 339, 1119–1148.
- [21] ROBBINS, H. & MONRO, S. (2011) A Stochastic Approximation Method *Ann. Math. Statistics* 22 (1951), 400–407. MR 42668
- [22] ROOSTA-KHORASANI, F. & MAHONEY, M. W. (2016) Sub-Sampled Newton Methods I: Globally Convergent Algorithms, *arXiv:1601.04737*
- [23] SAWARAGI, Y., NAKAYAMA, H. & TANINO, T. (1985) Theory of multiobjective optimization, *Elsevier*, MR 807529
- [24] SERAFINO, D., KREJIĆ, N., KRKLEC JERINKIĆ, N. & VIOLA, M. (2023) LSOS: Line-search Second-Order Stochastic optimization methods for nonconvex finite sums *Math. Comp*, 92, 1273-1299
- [25] SUN, S. & NOCEDAL, J. (2023) A trust region method for noisy unconstrained optimization. *Math. Program*, 202, 445–472

- [26] THOMANN, J. & EICHFELDER, G. (2019) A trust region Algorithm for Heterogeneous Multiobjective Optimization, *SIAM Journal on Optimization*, 29, 1017 - 1047.
- [27] VILLACORTA, K.D.V., OLIVEIRA, P.R. & SOUBEYRAN, A, (2014) A trust region Method for Unconstrained Multiobjective Problems with Applications in Satisficing Processes, *J Optim Theory Appl*, 160, 865-889.
- [28] YOUSEFI, M. & CALOMARDO, Á. M. (2022) A stochastic nonmonotone trust region training algorithm for image classification *16th International Conference on Signal-Image Technology and Internet-Based Systems (SITIS)* pp. 522-529